Grading studies for efficient Thermoelectric devices using combined 1D material and device modelling

P. Ponnusamy[1*], H. Naithani[1], E. Müller[1,2,3] and J. de Boor[1,4]

[1] German Aerospace Center (DLR), Institute of Materials Research, D–51170 Köln, Germany

[2] Justus Liebig University Giessen, Institute of Inorganic and Analytical Chemistry, Heinrich-Buff-Ring 17, D–35392 Giessen, Germany

[3] Justus Liebig University, Giessen, Center for Materials Research (ZfM/LaMa), Heinrich-Buff-Ring 16, D–35392 Giessen, Germany

[4] Faculty of Engineering, Institute of Technology for Nanostructures (NST) and CENIDE, University of Duisburg-Essen, Building BA, Bismarckstr. 81, D–47057 Duisburg, Germany

Corresponding authors : Prasanna Ponnusamy, Prasanna.ponnusamy@dlr.de; Johannes de Boor, Johannes.deboor@dlr.de

Abstract

The efficiency at which thermoelectric generators (TEG) can convert heat into electrical energy is governed by the properties of the employed functional materials. For a given thermoelectric (TE) material, efficiency needs to be maximized by adjusting e.g. the carrier concentration n. Usually, chemically homogeneous materials with a constant n along the leg are employed to fabricate TEG. However, for most TE materials the optimum n has a pronounced temperature dependence; typically increasing towards the hot side of the leg. A local variation of n, either continuously (grading) or discontinuously (segmenting) has thus the potential to increase the efficiency of TEGs substantially. Predictions on efficiency gain are challenging and an adequate physical model for the thermoelectric transport properties in the material *as well as* the device is required here. To address this challenge, we have combined a two-band model to describe the material properties with a device model based on the solution of the one-dimensional heat equation. Using Mg_2Sn as an example, we have adjusted the n profile to maximize the thermoelectric figure of merit locally. We show that this would result in an increase in

conversion efficiency by more than 7% for cold and hot side temperatures of 300 K and 700 K, respectively. Using thermoelectric self-compatibility criterion, we verify that the calculated n profile is indeed close to the best possible one. The presented methodology can be transferred to other material systems and we show that it can also be used to calculate the effect of other, practically more feasible n profiles.

1 Introduction

Thermoelectric (TE) devices convert thermal power into electrical power, or vice versa [1]. These are typically semiconductor materials and the material properties are temperature dependent. In order to estimate the performance of a TE material, a dimensionless figure of merit (zT) defined as $\frac{\alpha^2\sigma}{\kappa}T$, is commonly used where T is the absolute temperature, α the Seebeck coefficient, σ the electrical conductivity (reciprocal of the electrical resistivity ρ) and κ the thermal conductivity [1]. These three main TE properties are strongly coupled, implying a need to optimize them by e.g. tuning the carrier concentration n [2]. While the maximum of zT vs. n for a given temperature i.e., $\max(zT(n, T = \text{constant})$ (denoted by $zT_{\max,n}$), [3-12] has often been considered as a parameter to optimize material properties in general, and n in particular, it is clear [13-17] that optimum n obtained based on maximization of zT ($n_{\text{opt,zT}}(T) = \max_{\text{n}} \left(zT(n, T = \text{constant})\right)$) i.e., n corresponding to $zT_{\max,n}$ can be misleading for optimizing device properties. In order to avoid confusion, a look up table of all the nomenclature used in this work is provided in the Supplementary Information (SI). This is because device performance estimation requires consideration of the thermoelectric properties over the whole application temperature range and not at particular fixed temperatures.

To address this problem, we have previously employed efficiency (based on temperature dependent material properties) directly as a parameter for n optimisation using a combined material-device model [13, 14, 18]. The methodology was shown using $Mg_2(Si,Sn)$ solid solutions as an example. A Single Parabolic Band (SPB) model was used to model the material properties and it was confirmed that $n_{\text{opt,zT}}$ at e.g. the hot side (h) temperature is significantly different from the optimum n determined by maximizing efficiency over the temperature range of application $n_{\text{opt},\eta}(= \max_{\text{n}} \left(\eta(n, T_{\text{c}}, T_{\text{h}})\right))$ and the differences were quantified.

Usually, the zT of a thermoelectric material approaches its maximum in the temperature curve $zT(T)$ when minority carriers start to become excited to a significant extent and influence the

transport properties visibly and hence SPB model becomes unreliable here. To overcome this, at least a two-band model is required, one band to account for majority and minority carriers, each. This was done for a hypothetical n-type material in a recent publication by Beeckman *et al.* [19], where z at the average temperature of operation T_{m} ($T_{\mathrm{m}} = \frac{T_{\mathrm{h}}+T_{\mathrm{c}}}{2}$) was used as the parameter to be maximized. He concluded that $z(T_{\mathrm{m}})$ can be problematic as optimization target, in agreement with previous studies [20-22]. Since most of the n optimization studies use $n_{\mathrm{opt,zT}}(T)$ ($zT_{\mathrm{max,n}}$ at fixed temperatures to optimize n) [3-12], in our current work, we analyze the use $zT_{\mathrm{max,n}}$ at fixed temperatures and also the temperature averaged zT ($zT_{\mathrm{Tav}} = \frac{1}{T_{\mathrm{h}}-T_{\mathrm{c}}}\int_{T_{\mathrm{c}}}^{T_{\mathrm{h}}} z(T)T\,dT$, over the temperature range of application of the device) and compare with the results from using efficiency, using a realistic two band model.

In addition, the advantage of this combined material-device model is demonstrated by studying the effect of material grading and segmentation. Functional material grading involves tuning the material properties spatially along the arbitrary length (x) of the TE leg, to achieve a gain in functionality, power or efficiency [1, 22-25]. There have been some models to predict the gain in thermoelectric performance of such functionally graded materials [26-31], as well as several advanced experimental techniques that have practically made them feasible [23, 24, 32-35]. These models incorporate complex and sometimes unphysical models and don't clarify if an optimum grading has been reached.

While more complex grading is in principle feasible, the practically easiest is a mere optimization of the $n(x)$ profile as this can be achieved by tailoring the dopant concentration profile of the material. This leaves the material chemically quite homogeneous and also does not affect the lattice thermal conductivity a lot (if neglecting a minor effect due to point defect scattering). Here, grading is done using $n_{\mathrm{opt,zT}}(T)$ for each temperature (or position) along the length of the TE leg, and the corresponding local properties based on this $n_{\mathrm{opt,zT}}(T)$. In order to verify if such a graded material has the highest possible efficiency, the compatibility criterion [36-39] is checked.

In our study, we have chosen n-type Mg_2Sn as an example material since it is an end member of the Mg_2Si-Mg_2Sn solid solution series, a promising class of TE materials [40-42], and has received interest as a potential TE material due to its relatively high power factor for both n- and p-type material [42-45]. Furthermore, a two-parabolic-band model has been developed recently, which has been shown to predict the properties well [46-49]. Even though the method

is presented here for Mg_2Sn, it can be applied to any material system using suitable physical models to predict TE properties.

2 Method

The basic methodology of a combined material-device model was established in [14] using a SPB model. In the current study, a two-band model developed by H. Naithani *et al*. [49], for a more realistic modeling of the material properties including bipolar effects at high temperatures, is replacing the SPB model to adequately model the thermoelectric properties $\alpha(T,n), \sigma(T,n), \kappa(T,n)$ of Mg_2Sn; the relevant material parameters, the procedure and the equations are given in the SI. Using this model, it is straightforward to study the effects of different spatial profiles of n i.e., $n(x)$ profiles along the length of the TE leg.

The basic idea of segmenting and material grading (continuous segmentation) is presented schematically in Figure 1. A TE leg of length L connected to an external load resistor R_L is shown. When a temperature difference is applied, a temperature profile ($T(x)$) develops over the TE leg [21, 22]. This $T(x)$ is in principle non-linear due to the temperature dependence of κ as well as the Joule and Thomson effects [21, 22], but as discussed later and shown in SI (Figure S1), the deviation from linearity is relatively small. Since $n_{\mathrm{opt,zT}}$ varies with temperature, a gain in efficiency is possible when the *a priori* unknown optimum n is set along the length of the TE leg according to the temperature at each position in the leg. As η is a monotonous function of zT, choosing $n(x)$ according to the n that maximizes zT locally is a plausible strategy for grading. Since $T(x)$ is not far from linearity in a TEG, the temperature dependence in $n_{\mathrm{opt}}(T)$ can be translated directly into the required spatial dependence, i.e. $n(x) = \max_{\mathrm{n}} \left(zT(n,T(x))\right) =: n_{\mathrm{opt,zT}}(T(x))$ assuming a linear $T(x)$. For better accuracy, it is possible to find the $n_{\mathrm{opt,zT}}$ according to the exact $T(x)$ of the TE leg i.e., $n_{\mathrm{opt,zT}}(T(x))$, by iterating the calculation routine [50], required for materials with highly bent temperature profiles [51], however it is avoided here to minimize the computation time; results of iterated temperature profile are shown in the SI.

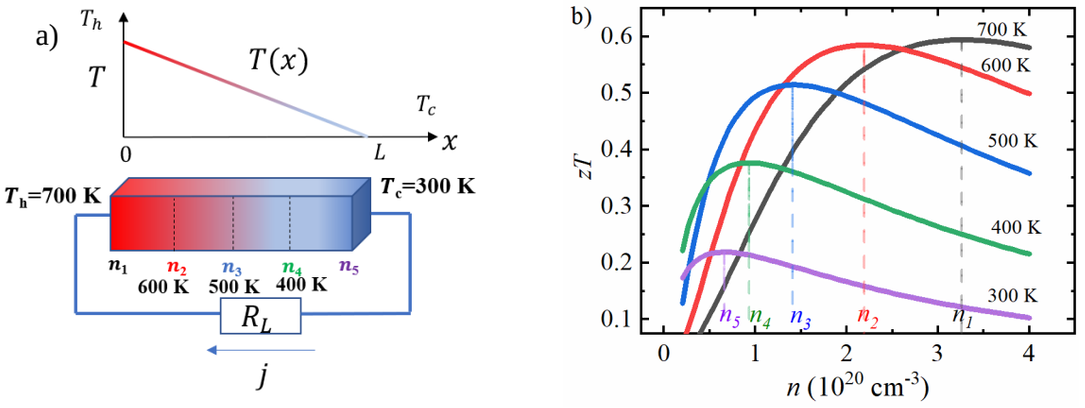

Figure 1: a) Schematic of a TE leg connected to an external load resistor R_L with an applied temperature difference $\Delta T = T_h - T_c$. Taking the shown linear $T(x)$ as a starting point, the $n(x)$ for a graded sample is chosen according to the $n_{opt,zT}(T(x))$(optimum n based on $zT_{max,n}$ for different T along the leg length). Here, fewer points are shown to demonstrate the idea of grading as a continuous segmentation. A continuously graded material has infinite such segments. For segmentation, $n_{opt,\eta}$ for each section i (e.g., $T_{h,s1}$=700K-$T_{c,s1}$= $T_{h,s2}$=600 K and so on) is used, b) Optimum n according to zT ($n_{opt,zT}$) is found for each T and the properties corresponding to $n_{opt,zT}(T)$ are set at each temperature point, dashed vertical lines indicate the corresponding optimum n.

For grading Mg_2Sn, zT vs. n characteristics at different temperatures are shown in Figure 1b. The obtained $n_{opt,zT}(T(x))$ profile is superimposed over the TE leg spatially and the properties corresponding to n_{opt} at that temperature then make up the spatially dependent properties of the graded material. For example, if $n_{opt,zT}$ is n_1 at 700 K as shown in Figure 1a, then $\alpha(700\ K) = \alpha(n_1)$ at 700 K and similarly $\alpha(n_2)$ at 600 K and so on, forming the temperature dependent properties of the graded TE leg; $n_{opt,zT}$ for intermediate temperatures are obtained by interpolation and employed accordingly.

Then, the efficiency and/or power output for this graded (or segmented) material is calculated using the iterative procedure described in [21], and compared with the homogeneous material. In steady-state, for a TE leg with a hot side temperature T_h and a cold side temperature T_c, $T(x)$ is obtained from eq. (1) [52, 53]

$$\frac{d}{dx}\left(\kappa\frac{dT}{dx}\right) - jT\frac{d\alpha}{dT}\frac{dT}{dx} = -\rho(T)j^2 \qquad (1)$$

where j is the current density. Here, $\frac{d}{dx}\left(\kappa\frac{dT}{dx}\right)$ corresponds to the local change of the Fourier heat flux considering the locally appearing Joule heat $\rho(T)j^2$ and Peltier-Thomson heat $T\frac{d\alpha}{dT}\frac{\partial T}{\partial x}$. The electrical power density (p) and efficiency (η) [21, 39] are then obtained as follows:

$$p = Vj \text{ and} \qquad (2)$$

$$\eta = p/q_{in} \text{ where} \qquad (3)$$

$$q_{in} = -\kappa_h\frac{dT}{dx_h} + j\alpha_h T_h\,. \qquad (4)$$

Here, voltage $V = V_o - R_{\text{in}}I$, $V_o = \int_{T_c}^{T_h} \alpha(T)dT$, internal resistance $R_{\text{in}} = \frac{1}{A}\int_0^L \rho\big(T(x)\big)dx$, A is the cross-sectional area. $\rho(T)$ the electrical resistivity of the TE material. The inflowing heat flux q_{in} at the hot side of the TEG leg is given by Eq. (4). $j\alpha_{\text{h}}\,T_{\text{h}}$ is the Peltier heat flux absorbed at the hot side. The maximum efficiency ($\eta_{\max}$) is obtained by setting $\frac{d\eta}{dj} = 0$.

3 Results and Discussion

3.1 Optimum carrier concentration

The pink curve in Figure 2 shows $n_{\text{opt,zT}}(T)$ obtained based on the results shown in Figure 1b. As a comparison, the $n_{\text{opt},\eta}$ for a homogeneous material [14, 21] (black curve) and zT_{TAv} (i.e. $n_{\text{opt},zT_{\text{TAv}}} = \max_{\text{n}} \big(zT_{\text{TAv}}(n, T_c, T_{\text{h}})\big)$, blue curve), for the considered temperatures as T_{h} with a constant T_{c} of 300 K is also shown. The pink curve thus shows the optimum n for a certain temperature, while the black and the blue curve that of a temperature interval.

It can be seen that $n_{\text{opt},\eta}(T_c, T_{\text{h}})$ is quite different from $n_{\text{opt,zT}}(T_{\text{h}})$ with a maximum relative overestimation of about 86% for T_{h} = 700 K; employing this $n_{\text{opt,zT}}$ in a homogeneous material would then lead to a reduction of the efficiency by 9%, compared to the efficiency resulting from $n_{\text{opt},\eta}(T_c, T_{\text{h}})$. For the same temperature interval (700 K to 300 K), comparing $n_{\text{opt},zT_{\text{TAv}}}$ with that of $n_{\text{opt},\eta}$, the relative difference is about 5%, which translates, however, only to a relative difference in efficiency of about 0.2%, showing that zT_{TAv} is useful as a parameter for optimization for this material. This has been found previously for this and other materials, but only in the temperature range where the SPB model can be employed [14].

It can also be seen from Figure 1b that the $n_{\text{opt,zT}}(T)$ varies quite a lot with T, providing us the opportunity to explore the potential of performance improvement by grading.

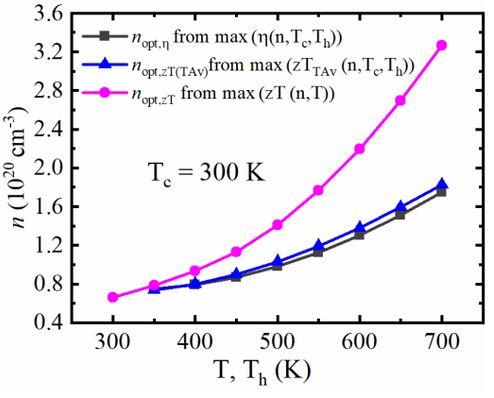

Figure 2: Optimum n according to different optimization parameters: $n_{\mathrm{opt,zT}}(T)$, $n_{\mathrm{opt},\eta}(T_\mathrm{h},T_\mathrm{c})$ and $n_{\mathrm{opt},zT_{\mathrm{TAv}}}(T_\mathrm{h},T_\mathrm{c})$ (for T_c = 300 K).

3.2 Material grading

A graded material is formed from $n_{\mathrm{opt,zT}}(T(x))$ having the material properties corresponding to n_{opt} at that particular T as explained before and is shown in Figure 3. The background lines correspond to the $n_{\mathrm{opt,zT}}(T)$ for $T = 300$ K to 700 K (in 50 K intervals). The points of intersection of the red curve (graded) and the background lines correspond to the $n_{\mathrm{opt,zT}}(T)$ at the respective T. For comparison, the material properties of a homogeneous material with $n =$ 1.75 $\times 10^{20}$ cm^{-3} (corresponding to $n_{\mathrm{opt},\eta}$ for T_h = 700 K and T_c = 300 K) is also shown (black curve with symbols). Figure 3d also shows a comparison of the spatially averaged zT, $zT_{\mathrm{SpAv}} = \frac{1}{L}\int_0^L zT(x)dx$, for homogeneous and graded material. To obtain the spatial averages, the exact temperature profiles obtained from the shown material properties are used. As might be expected, the largest differences in zT are observed towards the lower and upper temperature limit and zT_{SpAv} is 9% larger for the graded material. Consequently, a gain in efficiency of 7.3% can be obtained by such a material grading over the highest efficiency possible from a non-graded homogeneous material (Table 1).

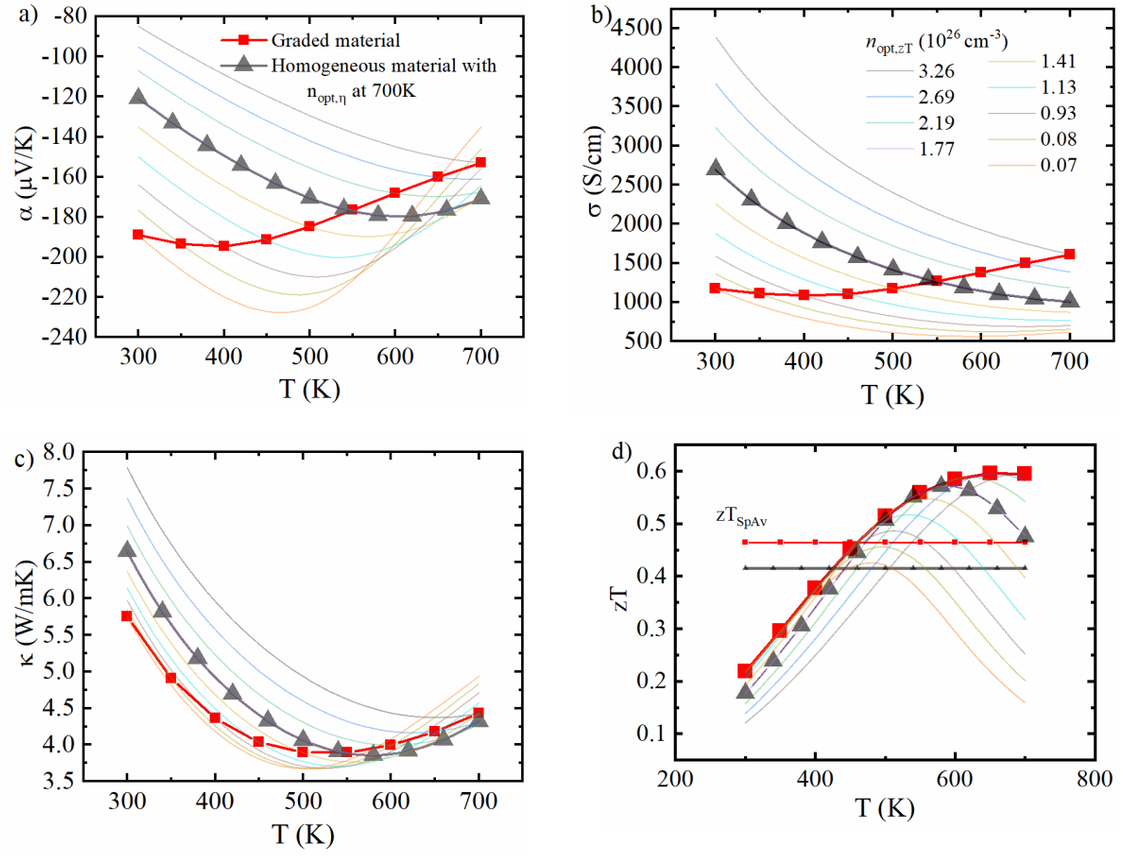

Figure 3: a) Seebeck coefficient; b) electrical conductivity; c) thermal conductivity and d) zT, for a graded material with $n_{\mathrm{opt},zT}(T)$ and the homogenous material with the optimum constant n for the full T range based on efficiency. The material properties of the graded material are obtained at each T from the $n_{\mathrm{opt,zT}}$ at that T.

It was shown previously that a graded material with a maximized $zT(T)$ does not necessarily give the highest possible efficiency [36] due to the limited self-compatibility of materials, i.e., due to incompatible heat vs. current flow. A strict optimization of $n(x)$ with respect to efficiency can be done mathematically as shown e.g. in [22, 26, 30, 31]. Here, we analyze the impact of compatibility on the material with the grading as obtained from $n_{\mathrm{opt,zT}}(T)$ following the approach from Snyder and Ursell [38]. For $T_{\mathrm{c}} = 300$ K and $T_{\mathrm{h}} = 700$ K, the reduced current density $u = \frac{j}{\kappa(T)\frac{dT}{dx}}$ is calculated as function of T. The current density j and $T(x)$ correspond to the maximum efficiency obtained for the graded material. In compatibility approach, the $u(T)$ is compared with the compatibility factor $s(T) = \frac{(-1+\sqrt{1+zT})}{\alpha T}$ [39]. If $u = s$ holds at any temperature, full self-compatibility of the leg is reached, i.e. the material contributes with its full potential to the efficiency of the device. Differing u and s correspond to a lower compatibility, limiting device efficiency. As shown in Figure 4a, u and s are not identical over the whole temperature range, but they are closer for the graded material compared to the homogenous material. We have calculated the reduced efficiency η_{r}, (for given hot and cold side temperature $\eta = \eta_{\mathrm{r}}\ \eta_{\mathrm{carnot}}$) given by [1, 39],

$$\eta_r = \frac{u(\alpha - u\rho\kappa)}{u\alpha + \frac{1}{T}} \tag{5}$$

and the η_{r} corresponding to u and s (maximum reduced efficiency) are shown in Figure 4b, showing almost perfect coincidence for graded material. The integral average of the relative difference in reduced efficiency i.e., $\frac{1}{\Delta T}\int_{T_c}^{T_h}(|\eta_{r,u}| - |\eta_{r,s}|)/|\eta_{r,u}|\, dT$ is a qualitative indicator for how close the employed $n_{\mathrm{opt,zT}}(T)$ matches to the ideal (unknown) $n(x)$ giving maximum efficiency. This relative difference calculated with u and s is about 0.8% for the graded material indicating that the $n_{\mathrm{opt}}(T)$ profile based on zT_{max} is very close, for this material and temperature conditions, to the maximum possible efficiency that can be obtained by $n(x)$ grading. For the homogeneous material, this difference amounts to about 2.9%, indicating that in addition to an increased overall zT in the graded material, the compatibility also improved. Given that the efficiency is a sub-linear function of zT, a 9% increase in zT_{SpAv} with grading does not scale to a corresponding increase in actual efficiency, highlighting the need for our exact performance calculation routine instead of the CPM. Considering a CPM TEG module

made of materials with zT corresponding to graded and homogeneous TE leg, a gain in efficiency of 6.44 % is predicted. Therefore, overall gain in efficiency in graded leg is mainly due to the increase in the effective zT of the graded leg, with a 0.8% gain in efficiency due to increased compatibility. Unlike previous studies on functional grading [22, 26, 30, 31] where compatiblity criterion has not been considered for such grading studies, our study shows that the chosen $n_{\mathrm{opt,zT}}(T)$ gives a close to maximum gain in efficiency based on self-compatibility for the considered material.

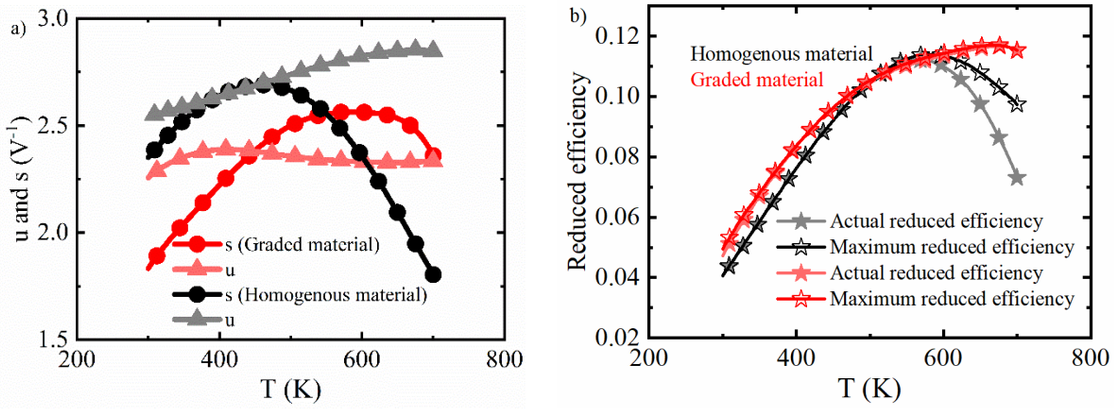

Figure 4: a) Variation of u and s with T for the graded and homogenous material. Maximum η_r is obtained locally when $u = s$ b) Actual η_r and maximum η_r for the graded and homogenous material. It can be seen that at higher temperatures, actual η_r is quite deviant from maximum η_r for homogenous material.

The combined material–device model employed here offers flexibility to check the effect of arbitrarily chosen $n(x)$ profiles on efficiency or power output. For example, the same study when performed with a linear grading following the equation $n = (-1.02985 \text{ x } 10^{26} + 5.64 \text{ x } 10^{23}\text{K}^{-1} \text{ x } T(x))\ \text{m}^{-3}$ (obtained using the endpoints with respect to temperature of $n_{\mathrm{opt,zT}}(T(x))$), results in a relative increase in efficiency of 5.3% compared to the homogeneous sample. Hence, if a material grading according to $zT_{\mathrm{max,n}}$ is not possible, a simple linear $n(T)$ grading can already give quite a gain in efficiency. Experimentally, graded Mg_2Sn (or $Mg_2(Si,Sn)$ might be obtained by annealing under a temperature gradient as Mg evaporation can tune the carrier concentration and is a highly temperature dependent process [54]. For example, by sintering together the powder stacks containing two different amounts of dopants corresponding to the optimum n, as presented e.g. in [55]. As the material remains highly doped and the change in carrier concentration is continuous, no interface or parasitic resistances is expected. When selecting a dopant species for practical implementation, the dopant diffusivity in the host material needs to be considered and highly mobile dopants as e.g. Ag for p-type Mg2Sn need to be avoided [56]. A possible dopant diffusion can most easily be monitored by

spatially resolved techniques, in particular measurements of the Seebeck coefficient by microprobe techniques [57, 58].

Additionally, the possibility of segmentation can be easily explored as well with such a model. For segmentation, the TE leg is divided into a number of sections along the length of the TE leg and $n_{\mathrm{opt},\eta}$ is obtained for each section considering the hot and cold side temperatures of that section. The material properties corresponding to $n_{\mathrm{opt},\eta}$ for each section are set. For example, if n_{s1} is the optimum n for a section 700 K-600 K, then α for the temperatures between 700-600 K is given by $\alpha(T(x), n_{s1})$ within that section. Here again, a linear $T(x)$ is assumed for calculation of the n_s values and hence, for this particular example, 500 K corresponds to the mid-point of the TE leg. For a Mg_2Sn leg with segments for the temperature intervals 700 K – 500 K and 500 K – 300 K, the $n_{\mathrm{opt},\eta}$ is found to be $n = 2.27 \times 10^{20}$ cm^{-3} and 0.98×10^{20} cm^{-3} respectively. The material properties corresponding to such a segmented TE leg are shown in the SI (Figure S2). As our model is based on the iterative integration method [21], it is straightforward to find the efficiency of such segmented leg. A gain in efficiency of 5.1% compared to the homogenous material is observed in such a TE leg which can be easily realized experimentally.

Table 1 summarizes the gain in efficiency of grading based on $n_{\mathrm{opt,zT}}(T(x))$, linear grading and two segmented leg, over the homogeneous leg.

Table 1: Efficiency and relative gain for differently graded legs for T_c =300 K and T_h=700 K.

	Homogeneous leg	Graded ($n_{\mathrm{opt,zT}}(T)$)	Linear grading $n = (-1.02985 \times 10^{26} + 5.64 \times 10^{23}\ \mathrm{K}^{-1} \times T(x))\ \mathrm{m}^{-3}$	Two segment leg with n_1= 2.27 $\times 10^{20}$ cm^{-3} and n_2= 0.98 $\times 10^{20}$ cm^{-3}
η_{max} (%)	6.85	7.35	7.21	7.20
Relative gain in efficiency	-	7.3	5.3	5.1

4 Conclusion

In summary, the advantages of using a simple and efficient combined material-device tool in optimizing performance has been shown using n-type Mg_2Sn as an example. Using a two band model the thermoelectric transport properties can be described over the full application temperature range and the effect of a locally varying $n(x)$ profile on the predicted conversion efficiency can easily be studied. Assuming a linear $T(x)$ and adjusting $n(x)$ such that zT is maximized at each position x, a gain in efficiency of 7.3% can be achieved in n-type Mg_2Sn, compared to the best homogeneous material with constant n. We furthermore show that an increase of about 5% can be achieved by using a simple linear $n(x)$ or by using a leg with two segments, which would be practically much easier to fabricate than a linearly graded or even non-linear $n(x)$. This paper not only shows possibilities to obtain gain in efficiency by material grading or segmentation but also considers the obtained results based on compatibility criterion. For Mg_2Sn, we find that grading according to the local zT also improves the self-compatibility of the material, increasing efficiency beyond the gain of the average zT. As the general temperature dependencies and interrelations between α, σ, κ are similar within the whole $Mg_2(Si,Sn)$ family it is plausible that the suggested approach is fruitful for that material class. Similar studies on other material systems can give a hint of the achievable gain in efficiency through such simple engineering.

Supplementary material:

The relevant two band model equations and other supporting graphs can be found in the Supplementary Material.

Acknowledgements

We would like to gratefully acknowledge the endorsement from the DLR Executive Board Member for Space Research and Technology and the financial support from the Young Research Group Leader Program. PP and HN would like to acknowledge the German Academic Exchange Service, DAAD (Fellowship No. 247/2017) for financial support.

Data Availability:

The data that supports the findings of this study are available within the article (and its supplementary material).

5 References:

1. Ioffe, A.F., et al., *Semiconductor thermoelements and thermoelectric cooling.* 1959. **12**(5): p. 42.
2. Snyder, G.J. and E.S. Toberer, *Complex thermoelectric materials.* Materials for sustainable energy: a collection of peer-reviewed research, 2011(review articles from Nature Publishing Group): p. 101-110.
3. Li, A., et al., *High-Performance Mg3Sb2-xBix Thermoelectrics: Progress and Perspective.* 2020. **2020**.
4. Toberer, E.S., A.F. May, and G.J. Snyder, *Zintl chemistry for designing high efficiency thermoelectric materials.* J Chemistry of Materials, 2010. **22**(3): p. 624-634.
5. Pei, Y., H. Wang, and G.J.J.A.m. Snyder, *Band engineering of thermoelectric materials.* 2012. **24**(46): p. 6125-6135.
6. Foster, S. and N. Neophytou, *Doping optimization for the power factor of bipolar thermoelectric materials.* Journal of Electronic Materials, 2019. **48**(4): p. 1889-1895.
7. Qin, F., et al., *Crystal Structure and Atomic Vacancy Optimized Thermoelectric Properties in Gadolinium Selenides.* 2020. **32**(23): p. 10130-10139.
8. Kang, S.D. and G.J. Snyder, *Transport property analysis method for thermoelectric materials: material quality factor and the effective mass model.* arXiv preprint arXiv:.06896, 2017.
9. Mao, J., et al., *Defect Engineering for Realizing High Thermoelectric Performance in n-Type Mg3Sb2-Based Materials.* Acs Energy Letters, 2017. **2**(10): p. 2245-2250.
10. McKinney, R.W., et al., *Search for new thermoelectric materials with low Lorenz number.* 2017. **5**(33): p. 17302-17311.
11. Hu, C., et al., *Transport mechanisms and property optimization of p-type (Zr, Hf) CoSb half-Heusler thermoelectric materials.* Materials Today Physics, 2018. **7**: p. 69-76.
12. Kumar, A., et al., *A Review on Fundamentals, Design and Optimization to High ZT of Thermoelectric Materials for Application to Thermoelectric Technology.* 2021: p. 1-23.
13. Ponnusamy, P., et al., *From basic transport properties to device efficiency: integrated performance prediction based on the Boltzmann transport equation*, in *VCT Virtual Thermoelectric Conference 2020*. 2020: Online.
14. Ponnusamy, P., et al., *Efficiency as a performance metric for material optimization in thermoelectric generators.* 2021.
15. Ioffe, A.F., *Physics of semiconductors*. 1960: Infosearch.
16. Ryu, B., J. Chung, and S. Park, *Thermoelectric efficiency has three Degrees of Freedom.* J arXiv preprint arXiv:.11148, 2018.
17. Kim, H.S., W.S. Liu, and Z.F. Ren, *The bridge between the materials and devices of thermoelectric power generators.* Energy & Environmental Science, 2017. **10**(1): p. 69-85.
18. Ponnusamy, P., et al., *Determining the optimal carrier concentrations and compositions in p-type magnesium silicide stannide using exact efficiency*, in *MSE Congress 2020*. 2020: Darmstadt, Deutschland.
19. Beekman, M., J.F. Ghantous, and K. Thomson, *Potential error from using ZT to optimize thermoelectric performance.* AIP Advances, 2021. **11**(5): p. 055207.
20. Kim, H.S., W. Liu, and Z. Ren, *The bridge between the materials and devices of thermoelectric power generators.* Energy & Environmental Science, 2017. **10**(1): p. 69-85.

21. Ponnusamy, P., J. de Boor, and E. Müller, *Using the constant properties model for accurate performance estimation of thermoelectric generator elements.* Applied Energy, 2020. **262**: p. 114587.
22. Goupil, C., *Continuum theory and modeling of thermoelectric elements*. 2015: John Wiley & Sons.
23. Mueller, E., et al., *Functionally graded materials for sensor and energy applications.* 2003. **362**(1-2): p. 17-39.
24. Shiota, I. and Y. Miyamoto, *Functionally graded materials 1996*. 1997: Elsevier.
25. Cramer, C.L., H. Wang, and K.J.J.o.E.M. Ma, *Performance of functionally graded thermoelectric materials and devices: A review.* 2018. **47**(9): p. 5122-5132.
26. Anatychuk, L. and L. Vikhor, *Computer design of thermoelectric functionally graded materials*, in *Functionally Graded Materials 1996*. 1997, Elsevier. p. 501-507.
27. Teraki, J. and T. Hirano, *A design procedure of functionally graded thermoelectric materials*, in *Functionally Graded Materials 1996*. 1997, Elsevier. p. 483-488.
28. Edry, I., et al. *Calculation of Temperature Profile and Power Perfomance of Thermoelectric Energy Materials*. in *2 nd European Conference on Thermoelectrics, Poland*. 2004.
29. Anatychuk, L. and L. Vikhor. *Physics and methods of FGTM design*. in *Proceedings ICT'03. 22nd International Conference on Thermoelectrics (IEEE Cat. No. 03TH8726)*. 2003. IEEE.
30. Kaliazin, A., V. Kuznetsov, and D. Rowe. *Rigorous calculations related to functionally graded and segmented thermoelements*. in *Proceedings ICT2001. 20 International Conference on Thermoelectrics (Cat. No. 01TH8589)*. 2001. IEEE.
31. Hirano, T., J. Teraki, and Y. Nishio. *Computational design for functionally graded thermoelectric materials*. in *Materials science forum*. 1999. Trans Tech Publ.
32. Anatychuk, L. and L. Vikhor. *Functionally graded materials and new prospects for thermoelectricity use*. in *XVI ICT'97. Proceedings ICT'97. 16th International Conference on Thermoelectrics (Cat. No. 97TH8291)*. 1997. IEEE.
33. Guélou, G., et al., *Issues and opportunities from Peltier effect in functionally-graded colusites: From SPS temperature modeling to enhanced thermoelectric performances.* 2021. **22**: p. 100948.
34. Ma, T., et al., *Continuously graded doped semiconducting polymers enhance thermoelectric cooling.* 2021. **119**(1): p. 013902.
35. Yang, S.E., et al., *Composition-segmented BiSbTe thermoelectric generator fabricated by multimaterial 3D printing.* 2021. **81**: p. 105638.
36. Snyder, G.J. and T.S. Ursell, *Thermoelectric efficiency and compatibility.* Phys Rev Lett, 2003. **91**(14): p. 148301.
37. Snyder, G.J.J.A.p.l., *Application of the compatibility factor to the design of segmented and cascaded thermoelectric generators.* 2004. **84**(13): p. 2436-2438.
38. Ursell, T. and G. Snyder. *Compatibility of segmented thermoelectric generators*. in *Twenty-First International Conference on Thermoelectrics, 2002. Proceedings ICT'02.* 2002. IEEE.
39. Rowe, D.M., *Thermoelectrics handbook: macro to nano*. 2005, CRC press.
40. Zaitsev, V., et al., *Highly effective Mg 2 Si 1− x Sn x thermoelectrics.* 2006. **74**(4): p. 045207.
41. Liu, W., et al., *Convergence of conduction bands as a means of enhancing thermoelectric performance of n-type Mg 2 Si 1− x Sn x solid solutions.* 2012. **108**(16): p. 166601.
42. Sankhla, A., et al., *Experimental investigation of the predicted band structure modification of Mg2 X (X: Si, Sn) thermoelectric materials due to scandium addition.* 2019. **125**(22): p. 225103.

43. Zhu, Y., et al., *Thermodynamic criterions of the thermoelectric performance enhancement in Mg2Sn through the self-compensation vacancy.* Materials Today Physics, 2021. **16**: p. 100327.
44. Kim, S., et al., *Electronic structure and thermoelectric properties of p-type Ag-doped Mg2Sn and Mg2Sn1-xSix (x = 0.05, 0.1).* Journal of Applied Physics, 2014. **116**(15): p. 153706.
45. Kamila, H., et al., *Analyzing transport properties of p-type Mg 2 Si–Mg 2 Sn solid solutions: optimization of thermoelectric performance and insight into the electronic band structure.* 2019. **7**(3): p. 1045-1054.
46. Kutorasinski, K., et al., *Importance of relativistic effects in electronic structure and thermopower calculations for Mg 2 Si, Mg 2 Ge, and Mg 2 Sn.* 2014. **89**(11): p. 115205.
47. Liu, W., et al., *New insight into the material parameter B to understand the enhanced thermoelectric performance of Mg 2 Sn 1− x− y Ge x Sb y.* 2016. **9**(2): p. 530-539.
48. Bahk, J.-H., Z. Bian, and A.J.P.R.B. Shakouri, *Electron transport modeling and energy filtering for efficient thermoelectric Mg 2 Si 1− x Sn x solid solutions.* 2014. **89**(7): p. 075204.
49. Naithani, H., E. Müller, and J. De Boor, *Developing a two-parabolic band model for thermoelectric transport modelling using Mg2Sn as example.* In preparation, 2021.
50. Helmers, L., et al., *Graded and stacked thermoelectric generators—numerical description and maximisation of output power.* 1998. **56**(1): p. 60-68.
51. Pei, Y., et al., *High thermoelectric figure of merit in heavy hole dominated PbTe.* Energy and Environmental Science, 2011. **4**(6): p. 2085-2089.
52. Domenicali, C.A., *Stationary temperature distribution in an electrically heated conductor.* Journal of Applied Physics, 1954. **25**(10): p. 1310-1311.
53. Domenicali, C.A., *Irreversible thermodynamics of thermoelectric effects in inhomogeneous, anisotropic media.* J Physical Review, 1953. **92**(4): p. 877.
54. Sankhla, A., et al., *On the role of Mg content in Mg2 (Si, Sn): Assessing its impact on electronic transport and estimating the phase width by in situ characterization and modelling.* 2021. **21**: p. 100471.
55. Noguchi, T., K. Takahashi, and T. Masuda, *Trial manufacture of functionally graded Si-Ge thermoelectric material*, in *Functionally Graded Materials 1996*. 1997, Elsevier. p. 593-598.
56. Ayachi, S., et al., *On the relevance of point defects for the selection of contacting electrodes: Ag as an example for Mg2(Si,Sn)-based thermoelectric generators.* Materials Today Physics, 2021. **16**: p. 100309.
57. Ziolkowski, P., et al., *Probing thermopower on the microscale.* Physica Status Solidi a-Applications and Materials Science, 2013. **210**(1): p. 89-105.
58. Kamila, H., et al., *Synthesis of p-type Mg2Si1-xSnx with x = 0-1 and optimization of the synthesis parameters.* Materials Today: Proceedings, 2019. **8**: p. 546-555.

AIP Publishing

Journal of Applied Physics

ACCEPTED MANUSCRIPT

PLEASE CITE THIS ARTICLE AS DOI: 10.1063/5.0089762

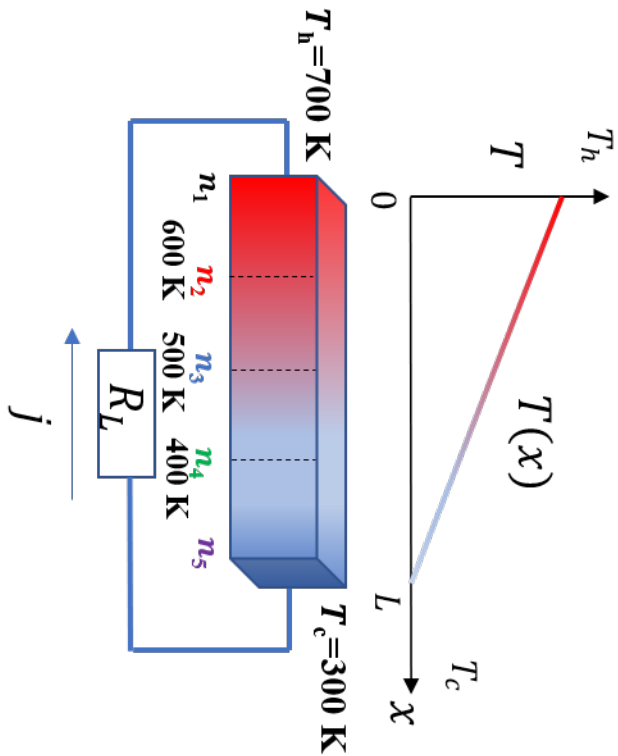

AIP Publishing

Journal of Applied Physics

ACCEPTED MANUSCRIPT

PLEASE CITE THIS ARTICLE AS DOI: 10.1063/5.0089762

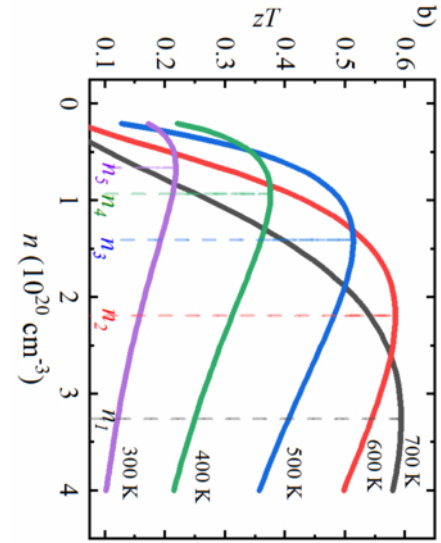

AIP Publishing

Journal of Applied Physics

ACCEPTED MANUSCRIPT

This is the author's peer reviewed, accepted manuscript. However, the online version of record will be different from this version once it has been copyedited and typeset.
PLEASE CITE THIS ARTICLE AS DOI: 10.1063/5.0089762

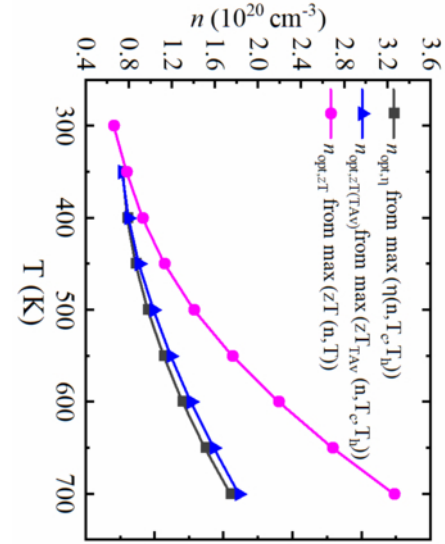

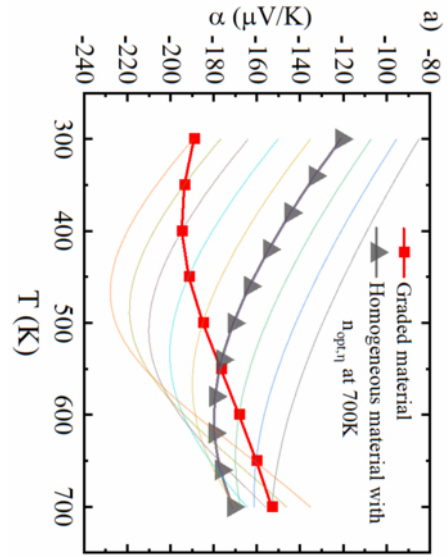

AIP Publishing

Journal of Applied Physics

ACCEPTED MANUSCRIPT

PLEASE CITE THIS ARTICLE AS DOI: 10.1063/5.0089762

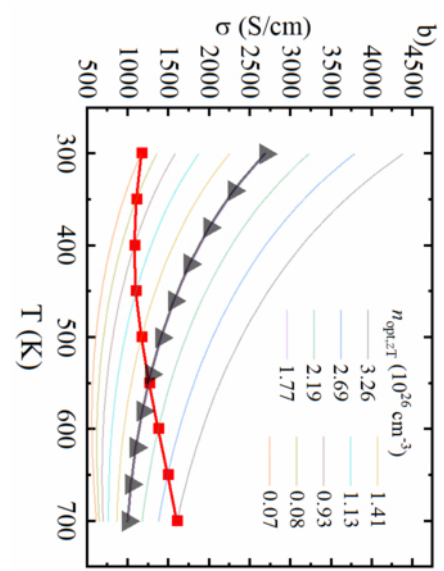

Journal of Applied Physics

PLEASE CITE THIS ARTICLE AS DOI: 10.1063/5.0089762

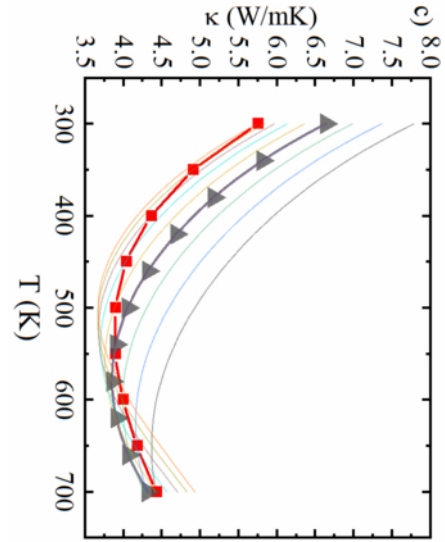

PLEASE CITE THIS ARTICLE AS DOI: 10.1063/5.0089762

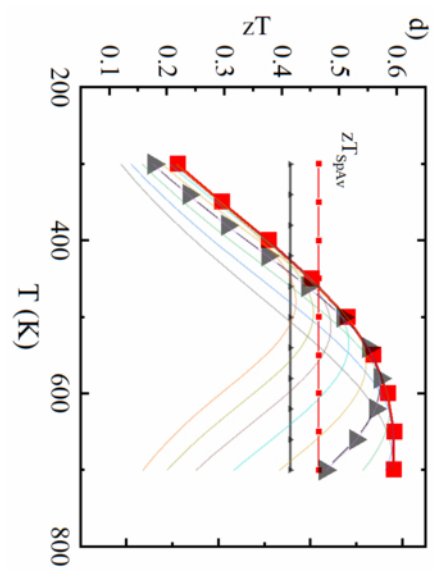

AIP Publishing

Journal of Applied Physics

ACCEPTED MANUSCRIPT

PLEASE CITE THIS ARTICLE AS DOI: 10.1063/5.0089762

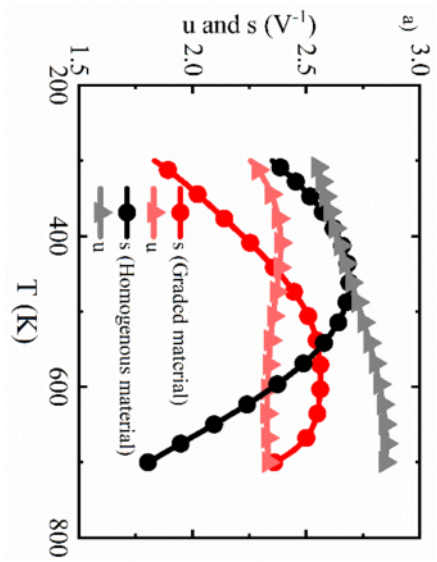

Journal of Applied Physics

PLEASE CITE THIS ARTICLE AS DOI: 10.1063/5.0089762